UDC 621.315.61 https://doi.org/10.20998/2074-272X.2024.1.09

O.O. Palchykov

Determination of the maximum mechanical stresses in the insulating material around a defect with a high dielectric permittivity in an electrostatic field

Introduction. *All insulating macrohomogeneous solid materials change shape under the influence of an electric field.* ***Problem.*** *The presence of minor defects changes the distribution of an electric field and causes a significant concentration of mechanical stresses in a given section of the material, which, under certain circumstances, can cause partial or complete destruction of this material.* ***Goal.*** *The purpose of the work is to determine maximum mechanical stresses according to the von Mises criterion in insulating materials around defects with ionized air and water in an electrostatic field. Also, to analyze the influence of the following parameters on the indicated stresses: the location of the defect, the orientation angle of the semi-major axis of the defect cross-section, the ratio of semi-major and semi-minor axes, elastic and dielectric properties of the insulating material and the defect.* ***Methodology.*** *The study is based on the interrelated equations of electrostatics and structural mechanics for an isotropic piecewise homogeneous medium. The solution of these equations is obtained by the finite element method.* ***Results.*** *Graphs of dependences of maximum mechanical stresses on the ratio of semi-major and semi-minor axes of the ellipsoidal cross-section of the defect have been obtained. The minimum ratio of the greatest stresses in the insulating materials around the surface cracks and pores for ionized air has been 9.3 times for the maximum ratio of major and minor semi-axes of the cross-section of the defect considered in the work, which is 10. For a water defect, the similar ratio has been 2...5.6 times, increasing when the relative dielectric permittivity of the insulating material changes from 7 to 2. When Young's modulus of the insulating material increases from 1 MPa to 100 GPa, the angles of the inclination of the linearized dependences of maximum mechanical stresses around bounded pores with ionized air (water) to the axis of the ratio of major and minor semi-axes of the defect cross-section have been increased by 35.9° (58.0°) and 18.6° (20.1°) at orientations of major semi-axes at angles of 0° and 45°, respectively.* ***Originality.*** *The numerical-field mathematical two-dimensional model has been developed for the first time, which consists of sequentially solved equations of electrostatics and structural mechanics, for the determination of the distribution of mechanical stresses in an insulating material with a liquid or gaseous defect. It has been established for the first time that the ratio of the elastic properties of the insulating material and the defect determines the angle of the inclination of the linearized dependence of the maximum mechanical stress to the axis of the ratio of major and minor semi-axes of the defect cross-section.* ***Practical value.*** *The types of defects that contribute to the aging of insulation materials under the combined action of an electric field and a stress field to the greatest extent have been established.* References 28, table 1, figures 10.

Key words: **insulating material, internal and surface defect, electrostatics, structural mechanics, von Mises stress, finite element method.**

В роботі методом скінченних елементів розроблено двовимірну математичну модель розрахунку розподілу механічних напружень під дією електростатичного поля в ізоляційному матеріалі з дефектом. Модель являє собою послідовно розв'язувані задачі електростатики та структурної механіки. У якості матеріалу дефекту виступали іонізоване повітря і вода. Розглядалися варіанти з внутрішніми та поверхневими дефектами, з врахуванням і без пружних властивостей дефекту. Поле механічних напружень розраховувалось на основі критерію фон Мізеса. Встановлено, що мінімальне відношення найбільших напружень в ізоляційних матеріалах з поверхневими тріщинами і порами для іонізованого повітря склало 9,3 рази для максимального співвідношення півосей поперечного перерізу дефекту 10. Для водного дефекту аналогічне відношення склало 2…5,6 разів, збільшуючись при зміні відносної діелектричної проникності ізоляційного матеріалу від 7 до 2. Визначено, що при збільшенні модуля Юнга ізоляційного матеріалу від 1 МПа до 100 ГПа кути нахилу до вісі лінеаризованих залежностей максимальних механічних напружень навколо обмежених пор з іонізованим повітрям (водою) збільшуються на 35,9° (58,0°) і 18,6° (20,1°) при орієнтаціях великих півосей під кутами 0° і 45° відповідно. Бібл. 28, табл. 1, рис. 10.

Ключові слова: **ізоляційний матеріал, внутрішній і поверхневий дефект, електростатика, структурна механіка, механічні напруження за фон Мізесом, метод скінченних елементів.**

Introduction. Solid, technically clean insulating materials have imperfections, a defective structure. Defects may have a technological or operational nature of origin. Structural micro-heterogeneity of solid insulating materials is confirmed by effective methods [1-4]. All insulating materials at the micro level change shape under the influence of an electric field. The presence of minor defects changes the distribution of electric field strength and creates a significant concentration of mechanical stresses in a given area of the material, which under certain circumstances can cause its partial or complete destruction. The most significant mechanical stresses are detected when the dielectric permittivity of the insulating material and the material defect differ sharply, for example, when the volume of the defect is filled with water or ionized air, for example, as a result of a partial discharge caused by high electric field strength.

Analysis of publications. The regularities of the distribution of the electrostatic field in insulating materials were considered in [5-10]. When covering the topic in [5], it would be worthwhile to reveal other shapes of defects, for example, with an ellipsoidal cross section, as well as to investigate the effect on the detection of dielectric breakdown of the inhomogeneity of the location of pores. The drawback in [6] is the lack of determination of the correlation between the increase in the electric field strength concentration and the experimental decrease in the breakdown voltage, as was done in [5]. Also, the shortcomings of this work include the failure to take into account air defects in the model, which are replaced by water coming from the environment. In [7], when studying the effect of defects on the linear capacity of the insulation, the compensatory effect of defects of different

nature is not taken into account, for example, a combination of local thinning and an internal defect with a lower dielectric permittivity than in the insulating material. With this effect, the linear capacity may not change much, although the concentration of the electric field will be significantly different from the average. The disadvantages of the work [8] are insufficient justification of the choice of shape and placement of air and water inclusions, which can affect the results of the work. Also, in [8], the volume of insulating material before and after seepage and after was taken unchanged, which is evident, in my opinion, not entirely correct. The results in [9] may be affected by the failure to take into account other orientations of the defect with a triangular cross section. The disadvantage in [10] is that the accuracy of the calculation of the electric field based on the neural network decreases when the parameters sought are far from the parameters of the numerical finite element model that participated in the training. The classic approach to considering the influence of the ionized region on the mechanical strength of the insulating material is based on Griffith criteria [11, 12]. The results of work [11] refer only to metal inclusion, the probability of which in modern insulation is rather insignificant. The shortcomings of the work [11] can also include the neglect of the elastic properties of the defect, as well as the lack of the consideration of the issue of the orientation of the defect at an angle of 45° to the area of the electrodes. Horovyts [12] considered surface cracks perpendicular to the electrode area in a 2D and axisymmetric formulation. The disadvantages in [12] are the lack of calculation of the field of mechanical stresses, that is, there is no understanding of the size of the area of stress concentration, and all the possible options for the orientation of the surface crack are not considered.

Stark and Garton made additions to the theory of mechanical stresses taking into account the plastic deformations of the dielectric to explain its destruction [13]. The failure criterion obtained by them corresponds to the minimum deformation when the collapse of the dielectric thickness occurs. A more general model for considering plastic deformation in polymers is presented in [14]. The common drawback of these models, in my opinion, is their one-dimensionality, which does not allow taking into account the Poisson effect. The work [15] presents a model of the formation of a nucleus and the growth of a conductive channel based on the energy principle, taking into account electric and mechanical fields, as well as the chemical potential at the interface between a conductive defect and a dielectric. However, the phenomenological parameter for determining the minimum possible size of a conductive nucleus, obtained from the study of the energy surface, is not supported by a physical assessment of its boundary (for example, how this parameter depends on the mechanical stresses at the boundary of the two-phase distribution).

In [16, 17], the possibilities of the formation of defects and dendrites under the action of electromechanical and mechanical forces, respectively, were investigated. In the model [16] there are parameters that cannot be directly determined, and therefore their value is determined only by the need to match the theoretical and experimental durability times of polyethylene insulation. In [17], there is no numerical assessment of the size of the defect and the electric field in it, which may affect the validity of the dendrite growth mechanism proposed in the work. In [18, 19], the growth patterns of dendrites under the influence of electric voltage were considered with the involvement of the concepts of Maxwell's stress tensor and fracture mechanics. In [18] it was established that the pre-channel structures are not caused by partial discharges, but an explanation of their occurrence by electromechanical stresses and shock ionization is proposed. The last mechanism is not considered in the work. Minor shortcomings in [18] when determining the field of mechanical stresses are the lack of consideration of the change in the density of the dendrite material (which was established experimentally in the work), as well as the arbitrary choice of the conductivity of the dendrite walls. The disadvantage of the work [19] is that the electromechanical forces are not calculated during the growth of the dendrite, but are only estimated by the rate of energy release.

The work [20] developed a model for determining mechanical stresses in polyethylene insulation with an ellipsoidal defect, the minor axis of which is parallel to the plane of the electrodes. The publication [21] developed a mathematical model for calculating the electric field, associated forces and mechanical stresses in the area of microdefects of polyethylene insulation in an axisymmetric formulation. A multiphysics 3D model that takes into account electric, thermal, and mechanical fields in the area of water treeings is presented in [22]. The common shortcomings of the works [20-22] are the consideration of only one orientation of the defect (which, in turn, is not the most likely), failure to take into account the elastic properties of the defect, insufficient justification of the choice of electrical properties of the defect, partiality of the study (only polyethylene is considered).

An experimental study of the influence of the level of irradiation by accelerated electrons with energy of 0.5 MeV as a result of technological manufacturing on the mechanical and electrical characteristics of cable insulation was carried out in [23]. Despite the high level of research, there is no theoretical explanation of the strong correlation between the mechanical and electrical characteristics of radiation cross-linked insulation in [23]. In [24], a model for calculating the electric field in three-component insulation, modeled as a two-layer tape, is proposed. It would be worth comparing this model with the numerical field model, which consists of a fiberglass base, an impregnation composition, and a mica paper tape. The authors of the work [25] justified the effectiveness of detecting technological defects in high-voltage insulation based on the characteristics of partial discharges in gas inclusions. In [25] there is no comparison of the proposed chain model with the numerical field model, and there is also a question about the shape of the defect.

In [26], various criteria for the destruction of polymers (and in the general case of porous materials, including composite materials, wood, metals) were

analyzed and it was shown that all criteria can be reduced to the von Mises criterion with some error. The disadvantage is that the introduction of new failure criteria, in addition to the von Mises and Tresca criteria, requires additional parameters that are determined experimentally for a specific material, which reduces their universality.

Thus, at the moment, the existing mathematical models do not allow to calculate the maximum mechanical stresses for solid insulation with a liquid or gaseous defect in a 2D formulation and to determine them depending on the ratio of the semi-axes of the cross section of the defect, the orientation of the defect, as well as when changing the elastic and dielectric properties of the insulation material and defect within wide limits.

General characteristics of work. The goal of the work is to determine the maximum mechanical stresses according to the von Mises criterion in insulating materials around defects with ionized air and water in an electrostatic field. To analyze the influence of the following parameters on the indicated stresses: the location of the defect, the orientation angle of the semi-major axis of the cross-section of the defect and its relation to the minor semi-axis, elastic and dielectric properties of the insulating material and the defect.

The relevance of the work is related to the theoretical explanation of the heterogeneity of the microstructure of insulating materials, as well as the identification of the features and reasons for the development of micro-sized air/water cavities and treeing formations in such materials.

Object of study. In the work, the pore in the volume of the dielectric is modeled in cross-section as an ellipse, and the crack on the surface of the dielectric is modeled as half an ellipse. The computational domain in the case of a pore is a rectangle with sides $10a$ and $14a$, where a is the semimajor axis of the ellipse. The minor semi-axis of the ellipse is defined as $b = a/k$, where k is the parameter that lies within $k \in [1...10]$. The computational domain in the case of a crack is a rectangle with sides $10a$ and $7a$. The distance between the electrodes in the first case is the larger side of the rectangle, in the second case it is the smaller side. The dimensions of the computational domain are chosen so that on its boundaries the modulus of the electric field strength vector approaches the values of the modulus of the strength vector in the insulating material without a defect. Three cases of ellipse and semi-ellipse arrangement were considered in the work: at angles of 0°, 45°, and 90° between the semi-minor axis and the plane of the electrode. Options of through and limited pore were also considered. In the first case, the elastic properties of the material of the defect can be neglected. In the second case, we mean a rather long cylindrical volume in the direction perpendicular to the computational domain, bounded on both sides by parallel planes. The elastic properties of the material of this volume should affect the distribution of mechanical stresses in the insulating material.

Mathematical model. The calculation of electromechanical forces is based on the coupled solution of the equations of electrostatics and structural mechanics developed for an isotropic piecewise homogeneous medium with linear properties in a 2D formulation [27, 28]:

$$\nabla^2\varphi = 0;$$

$$\boldsymbol{E} = -\nabla\varphi;$$

$$\boldsymbol{D} = \varepsilon_0\varepsilon_{ri(d)}\boldsymbol{E};$$

$$\nabla\boldsymbol{\sigma} = 0; \quad (1)$$

$$\boldsymbol{\varepsilon} = 0{,}5[(\nabla\boldsymbol{u})^{\mathrm{T}} + \nabla\boldsymbol{u}]; \quad (2)$$

$$(\sigma_{xx}\ \sigma_{yy}\ \sigma_{zz}\ \sigma_{xy})^T = C_M(\varepsilon_{xx}\ \varepsilon_{yy}\ \varepsilon_{zz}\ \varepsilon_{xy})^T, \quad (3)$$

where φ is the scalar electrostatic potential; $\boldsymbol{E}$ is the electric field strength vector; $\boldsymbol{D}$ is the electric induction vector; ε_0 is the electrical constant ($8.854\cdot10^{-12}$ F/m); $\varepsilon_{ri(d)}$ is the relative dielectric permittivity of the insulating material (defect); $\boldsymbol{\sigma}$ is the tensor of mechanical stresses; $\boldsymbol{\varepsilon}$ is the strain tensor; $\boldsymbol{u}$ is the vector of displacements of the body (the difference between the coordinates of the final and initial position of each point); σ_{ij}, ε_{ij} are the components of mechanical stress and strain tensors, respectively; C_M is the elasticity matrix, which is written through Young modulus E_M and Poisson ratio ν for an isotropic material in the form:

$$C_M = \frac{E_M}{(1+\nu)\cdot(1-2\nu)}\begin{pmatrix} 1-\nu & \nu & \nu & 0 \\ \nu & 1-\nu & \nu & 0 \\ \nu & \nu & 1-\nu & 0 \\ 0 & 0 & 0 & 0{,}5(1-2\nu) \end{pmatrix}.$$

It is convenient to write the elasticity matrix for gas and liquid inclusion in terms of the shear modulus G and the volumetric modulus of elasticity K:

$$C_M = \begin{pmatrix} K+\frac{4G}{3} & K-\frac{2G}{3} & K-\frac{2G}{3} & 0 \\ K-\frac{2G}{3} & K+\frac{4G}{3} & K-\frac{2G}{3} & 0 \\ K-\frac{2G}{3} & K-\frac{2G}{3} & K+\frac{4G}{3} & 0 \\ 0 & 0 & 0 & G \end{pmatrix}.$$

According to [27], all volume forces are reduced to surface forces and are taken into account due to boundary conditions.

The specific force per unit surface area of the insulating material f_s is calculated on the basis of the Maxwell stress tensor [28] as

$$f_s = (\boldsymbol{D}_2\cdot\boldsymbol{n}\cdot\boldsymbol{E}_2 - \boldsymbol{D}_1\cdot\boldsymbol{n}\cdot\boldsymbol{E}_1) - 0{,}5(\boldsymbol{D}_2\cdot\boldsymbol{E}_2 - \boldsymbol{D}_1\cdot\boldsymbol{E}_1)\cdot\boldsymbol{n}, \quad (4)$$

where $\boldsymbol{n}$ is the external normal vector.

For liquids and gases, the shear modulus is zero, but for numerical implementation, $G = 0.2$ Pa was assumed. The volumetric elastic modulus of the defect in the case of a limited pore was taken as $K = 2.2$ GPa for water, and $K = 0.101$ MPa for ionized air.

Equations of structural mechanics (1)–(3) are written in the plane strain approximation [28], i.e. $\varepsilon_{xz} = \varepsilon_{yz} = \varepsilon_{zz} = 0$. Therefore, $\sigma_{xz} = \sigma_{yz} = 0$ and the elasticity matrix changes its dimension from 6×6 to 4×4.

Boundary conditions of the problem of electrostatics:

- for the lower plane $\varphi_1 = |\boldsymbol{E}_\infty|\cdot d$;
- for the upper plane $\varphi_2 = 0$;
- for the side surface $\boldsymbol{n}\cdot\boldsymbol{D} = 0$,

where $\boldsymbol{E}_\infty$ is the electric field strength vector in the insulating material in the absence of a defect; d is the distance between the upper and lower planes.

Boundary conditions of the structural mechanics problem:

- for the lower plane $\boldsymbol{u} = 0$;
- for the upper plane $\boldsymbol{\sigma}\cdot\boldsymbol{n} = f_s$.

At the interface of two media, the following are accepted: for the problem of structural mechanics, the equality of the displacement vectors, for the problem of electrostatics, Neumann boundary conditions.

The main assumptions made in the model are: the insulating material has no conductivity; charges at the interface of dielectric media are absent, as well as volume charges; there are no mechanical stress components caused by thermal and gravitational fields; when the volume changes, the physical properties of the materials do not change and there is no associated polarization; small deformations of the studied sample (for example, the maximum deformation was calculated for rubber in pre-breakthrough fields, which was 2.4 %; for polyimide film – 0.049 %). The latter involves considering the model only within the limits of the theory of linear elasticity, and also allows the coupled system of equations to be divided into two subproblems that are solved sequentially: the electrostatics problem for calculating the specific force, which is then used as a boundary condition for the structural mechanics problem. As a result of the linearity of the separately taken problems of electrostatics and structural mechanics, when the dimensions of the sample are changed in compliance with the above-mentioned boundary conditions, the values of the electric and mechanical fields change proportionally.

The distribution of mechanical stresses was calculated according to the von Mises criterion [28]

$$\sigma = 0{,}5^{0{,}5}\cdot[(\sigma_{xx} - \sigma_{yy})^2 + (\sigma_{yy} - \sigma_{zz})^2 + (\sigma_{zz} - \sigma_{xx})^2 + 6(\sigma_{xy})^2]^{0.5}.$$

Among such stresses the maximum value $\sigma_{\max}$ was founded, which was further presented in relative units:

$$\sigma^*_{\max} = \sigma_{\max}/[0{,}5\varepsilon_0\varepsilon_{ri}(\boldsymbol{E}_\infty)^2].$$

Therefore, without a defect, the relative mechanical stress according to von Mises is $\sigma^*_{\max} = 1$. The similarity of the forces (4) created by the electrostatic field based on Maxwell's stress tensor serves as a justification for the presentation of mechanical stresses in relative units.

The model is also characterized by the similarity of electrostatic fields when the permittivity of the insulating material changes, which is true when the condition $\varepsilon_{ri} << \varepsilon_{rd}$ is fulfilled. Mechanical stresses were studied at the relative dielectric permittivity of the insulating material within $\varepsilon_{ri} \in [2\ldots7]$, of the defect with water $\varepsilon_{rd} = 80.2$. Strongly ionized regions arising in the case of a partial breakdown were modeled by a material with a relative dielectric permittivity $\varepsilon_{rd} = 16000$ to adjust the numerical model [5]. This value was chosen for the purpose of practical implementation in the problem of electrostatics of the model of an ideal conductor with $\varepsilon_{rd} \to \infty$, as several times the value of the maximum dielectric permittivity of the materials in the model. The given model is numerically implemented using the finite element method in the COMSOL code. For a more general approach to the problem of mechanical stresses caused by an electric field, the problem is formulated in such a way as to take into account the mechanical and electrical properties of most electrical insulating materials (and even hypothetical values such as $E_M = 10^5$ MPa). The physical properties of some electrical insulating materials are given in Table 1. That is, based on the analysis of the properties of electrical insulating materials, the following ranges of parameter changes were chosen: relative dielectric permittivity $\varepsilon_{ri} = 2$–7; Poisson ratio $\nu = 0.1$–0.499; Young modulus $E_M = 1$–10^5 MPa.

Table 1

Physical properties of some electrical insulating materials

Material	Young's modulus E_M, MPa	Poisson ratio ν	Dielectric permittivity ε_{ri}
Rubber	0,5…8	0,47	2,6
Polyvinyl chloride	$(2{,}7\ldots4)\cdot10^3$	0,35…0,38	3,2
Polyimide film	$3\cdot10^3$	0,499	3,5
Cellulose	$(2{,}7\ldots6{,}5)\cdot10^3$	0,38…0,46	6,5
Electro-porcelain	$6\cdot10^4$	0,23	6…7

Research results. Examples of electric fields and mechanical stress fields in insulating materials ($\varepsilon_{ri} = 2$) at $|\boldsymbol{E}_\infty| = 40$ MV/m with variants of the water defect are shown in Fig. 1–3. The maximum concentration of mechanical stresses for the defect shown in Fig. 1,*b*, is located at some angle to the semi-major axis, which tends to decrease with an increase in the geometric ratio of the defect section. According to Fig. 1, the orientation of the areas of concentration of mechanical stresses promotes the growth of surface cracks with angles of 0°...45° between the minor semi-axis and the surface of the electrodes in the direction of the opposite electrode in the event that the mechanical stress exceeds the compressive strength limit of the insulating material. As can be seen from Fig. 2, 3, when changing the Young modulus of insulating materials, the maximum mechanical stress shifts. In the case presented in Fig. 2, the concentration of mechanical stresses decreases along the extension of the major semi-axis and increases along the minor axis. In the case of Fig. 3, the concentration of mechanical stresses with an increase in the Young modulus moves from a position above the semi-major axis to below it. For a limited water pore with a semi-major axis parallel to the plane of the electrodes and a circular limited pore, the zone of concentration of mechanical stresses with an increase in Young modulus turns by a jump of 90°.

For air ionized through pores, the zones of concentration of mechanical stresses are located: as rotated at a small angle clockwise relative to the major semi-axis for the defect region, similar to the image in Fig. 3,*d*; on an axis parallel to the plane of the electrodes for other cases of orientation of pores.

Figure 4 presents the results of calculating the maximum mechanical stresses depending on the orientation of the surface defect filled with ionized air, its geometric ratio and Poisson ratios of insulating materials. For variants of cracks with 0° and 45° orientation, the effect of Poisson ratio of the insulating material on the stress concentration around the defect is minimal. For the specified options, the dependencies for the material with $\nu = 0.1$ are presented. The difference in dependencies for defects in the insulating material with $\nu = 0.499$ is up to –3.5 %. Here, the specified models for determining the stress field are invariant to a change in Young modulus.

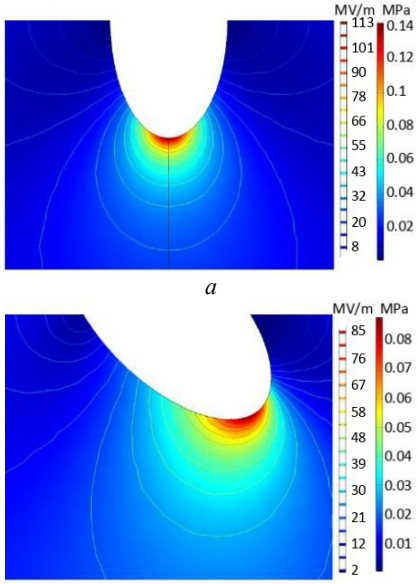

Fig. 1. Mechanical and electric fields around a surface water crack, the minor semi-axis of the cross-section of which is oriented at an angle of 0° (*a*) and 45° (*b*) to the plane of the electrodes in insulating materials with $\nu = 0.1$ regardless of Young modulus

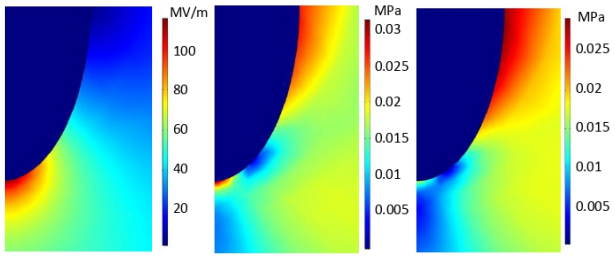

Fig. 2. Distribution of the modulus of the electric strength vector (a) and von Mises stresses for the cases of water limited pores in insulating materials with $\nu = 0.1$: $E_M = 1$ MPa (*b*), $E_M = 10^5$ MPa (*c*)

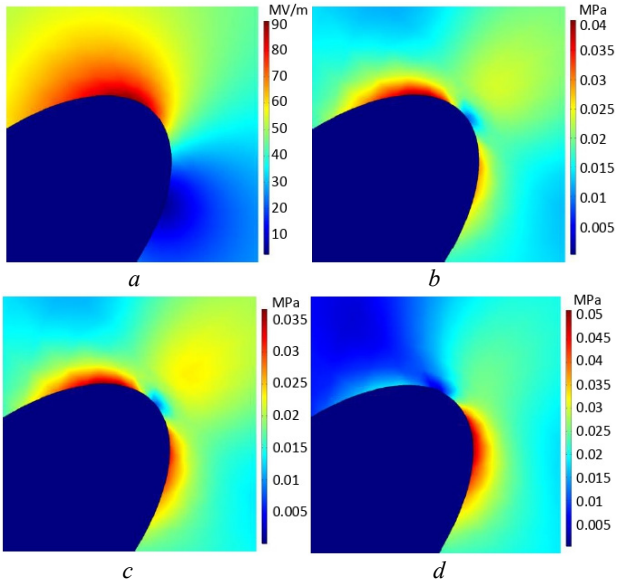

Fig. 3. Distribution of the electric strength vector modulus (*a*) and von Mises stresses for the cases of water limited pores in insulating materials with $\nu = 0.1$: $E_M = 1$ MPa (*b*), $E_M = 10^3$ MPa (*c*), $E_M = 10^5$ MPa (*d*)

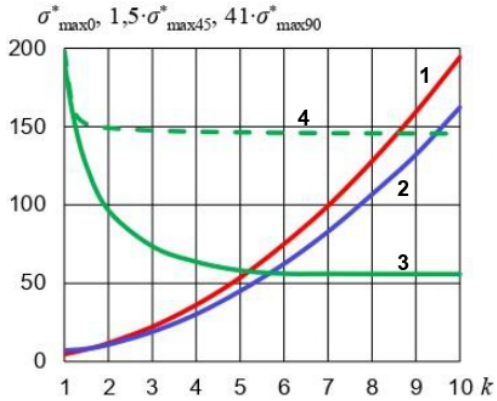

Fig. 4. Dependencies of the maximum mechanical stresses around surface cracks with ionized air, the minor semi-axis of which is oriented to the plane of the electrodes at angles of 0° (curve 1), 45° (curve 2), and 90° (curves 3 and 4 for materials with $\nu = 0.1$ and with $\nu = 0.499$, respectively), on the geometric ratio

Figures 5, 6 present the results of calculating the maximum mechanical stresses depending on the orientation of the cross-section of the pore filled with ionized air, its geometric ratio and the elastic properties of the insulating material.

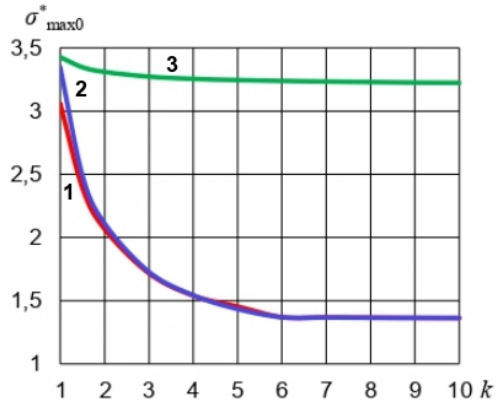

Fig. 5. Dependencies of the maximum mechanical stresses around pores with ionized air, the minor axis of which oriented to the plane of the electrodes at an angle of 0°, on geometric ratio for the cases of: a limited pore in a material with $\nu = 0.1$ and $E_M = 1$ MPa (curve 1); through pores in materials with $\nu = 0.1$ (curve 2) and with $\nu = 0.499$ (curve 3)

In Fig. 5, the stress graph in the material with $\nu = 0.1$ and $E_M = 10^5$ MPa coincides with the graph for the through pore in the material with the corresponding Poisson ratio. Also in Fig. 5 graph of stresses in materials with $\nu = 0.499$ and Young modulus in the range $[1...10^5]$ MPa coincides with the graph for a through pore in the material with the corresponding Poisson ratio. The maximum discrepancy by module in these cases was 1.1 %. Figure 6 for limited pores with an orientation of 45° in insulating materials with $E_M = 1$ MPa and Poisson ratio in the range [0.1...0.499] presents a graph constructed according to the data of the model with $\nu = 0.1$. The maximum differences in the modulus of stress mapping for the model with $\nu = 0.499$ amounted to 1.4 % and 10.9 % for $k \in [2\ldots10]$ and $k = 1$, respectively. In Fig. 6 graphs of stresses in materials with $E_M = 10^5$ MPa and Poisson ratios $\nu = 0.1$ and $\nu = 0.499$ coincide with the graphs for through pores

in materials with the corresponding Poisson ratio and the position of the defect with a maximum discrepancy of –0.54 %.

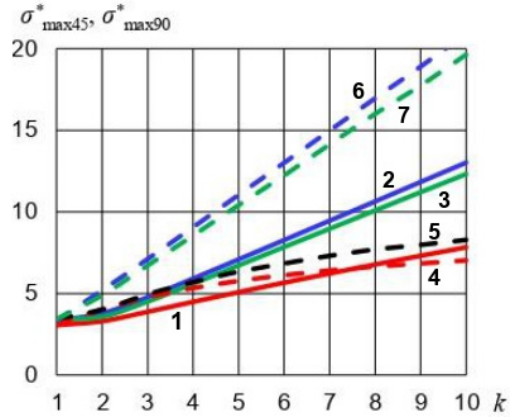

Fig. 6. Dependencies of the maximum mechanical stresses around pores with ionized air, the minor semi-axis of which oriented to the plane of the electrodes at angles of 45° (solid lines), 90° (dashed lines), on the geometric ratio for the cases: in materials with E_M = 1 MPa and ν = 0.1...0.499 (curve 1); in the material with E_M = 1 MPa and ν = 0.1 (curve 4); in the material with E_M = 1 MPa and ν = 0.499 (curve 5); for through pores in materials with ν = 0.1 (curves 2 and 6) and with ν = 0.499 (curves 3 and 7)

Figures 7, 8 present the results of calculating the maximum mechanical stresses depending on the orientation of the cross-section of the water pore, its geometric ratio and the elastic properties of insulating materials. Figure 7 does not show stress graphs in materials with ν = 0.1 and $E_M = 10^5$ MPa; ν = 0.499 and E_M = 1 MPa; ν = 0.499 and $E_M = 10^5$ MPa. These, as in the case of pores with ionized air, coincide with the graphs for through pores. The maximum discrepancy is 2.3 %. The dependences for materials with $E_M = 10^5$ MPa and ν = 0.499 when defects are oriented at angles of 45° and 90° coincide with those shown in Fig. 8 dependencies for the material with $E_M = 10^5$ MPa and ν = 0.1. The difference of dependencies for the range of change of the parameter $k \in [2...10]$, which determines the size of the defect, is modulo [4.9...1.2] %.

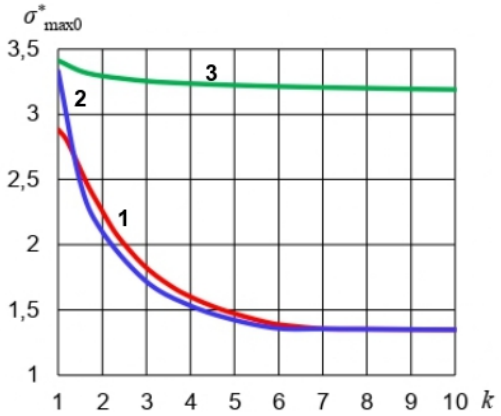

Fig. 7. Dependencies of the maximum mechanical stresses around water pores, the semi-minor axis of which is oriented to the plane of the electrodes at an angle of 0°, on the geometric ratio for the cases of: a limited pore in a material with ν = 0.1 and E_M = 1 MPa (curve 1); through pores in materials with ν = 0.1 (curve 2) and with ν = 0.499 (curve 3)

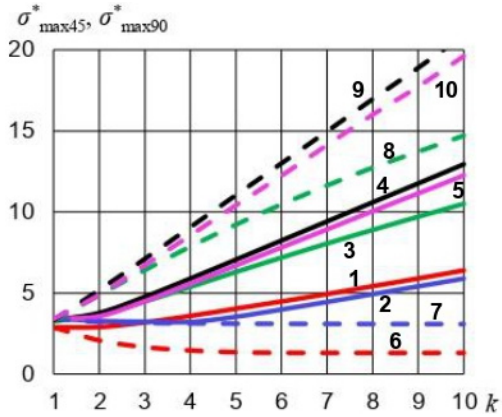

Fig. 8. Dependencies of maximum mechanical stresses around water pores, the minor semi-axis of which is oriented to electrode planes at 45° angles (solid lines), 90° (dashed lines), on the geometric ratio for the cases: in the material with E_M = 1 MPa and ν = 0.1 (curves 1 and 6); in the material with E_M = 1 MPa and ν = 0.499 (curves 2 and 7); in the material with $E_M = 10^5$ MPa and ν = 0.1 (curves 3 and 8); for through pores in materials with ν = 0.1 (curves 4 and 9) and with ν = 0.499 (curves 5 and 10)

For all considered through pores, changing the Young modulus of the insulating material has no effect on the pattern of stress distribution. It can be asserted about the practical identity of the dependencies of the maximum mechanical stresses in the region of defects with ionized air and water when their major semi-axis is oriented at the angle of 90° to the plane of the electrodes, as well as about the identity of stresses around through pores with ionized air and water at other angles. When the ratio of the major and minor semi-axes of the defect cross-section k increases from 1 to 10, the maximum mechanical stresses around limited and through pores with ionized air (water) when their major semi-axes are oriented to the plane of the electrodes at angles of 0° and 45° increase by 2.3...6.3 (0.5...6.3) and 2.6...3.9 (2.2...3.9) times, respectively.

During the study of the surface water defect, the lack of proportionality of the mechanical stresses with a change in the relative dielectric permittivity was revealed. This can be explained by the presence of a small electric field in the defect, which will change when the dielectric permittivity of the insulating material changes. And therefore the graphs shown in Fig. 9, 10, are constructed with defined relative mechanical stresses as follows: $\sigma^*_{maxw} = \sigma^*_{max}\varepsilon_{ri}$.

The graphs presented in Fig. 9, 10 are valid for insulating materials whose elastic properties vary widely. The average discrepancy of the dependences in Fig. 9 when the Poisson ratio changes in the range [0.1...0.499] is 3 %. According to Fig. 9 when the relative dielectric permittivity of the insulating material increases from 2 to 7 for the range of the ratio of the major and minor semi-axes of the defect section $k \in [1…10]$, the maximum mechanical stresses around the surface water cracks with the orientation of the minor semi-axes to the plane of the electrodes at angles of 0° and 45° decrease 1.1...3 times.

So, despite the identity of the distribution of the electric field for identical regions of the variants with external and internal defects, the distribution of the mechanical stress field is not the same, but depends on the

ratio of the elastic properties of the insulating material and the defect, the location of the defect.

Verification of the obtained results. The model was tested according to the numerical study of the work [20]. In the model given in [20], the problem was solved in an axisymmetric formulation, taking into account the direct current conductivity. For the adequacy of the comparison, the axisymmetricity of the problem and the complex dielectric permittivity were taken into account in the model developed in this work. The error for the maximum value of the mechanical stress in comparison with the result obtained in [20] was 0.12 %, which confirms the correctness of the numerical results of this work. In addition, according to the order of electrical and electromechanical quantities, the numerical results of this work and works [21, 22] coincide.

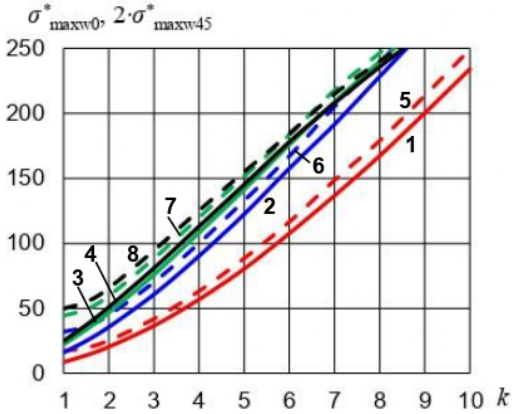

Fig. 9. Dependencies of the maximum mechanical stresses around surface water cracks, the minor semi-axis of which is oriented to the plane of the electrodes at angles of 0° (solid lines), 45° (dashed lines), on the geometric ratio for cases: $\varepsilon_{ri} = 2$ (curves 1 and 5), $\varepsilon_{ri} = 4$ (curves 2 and 6), $\varepsilon_{ri} = 6$ (curves 3 and 7), $\varepsilon_{ri} = 7$ (curves 4 and 8)

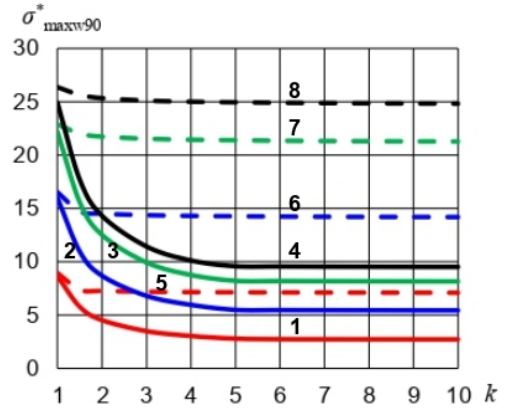

Fig. 10. Dependencies of the maximum mechanical stresses around surface water cracks, the minor semi-axis of which is oriented to the plane of the electrodes at an angle of 90°, on the geometric ratio in materials with $\nu = 0.1$ (solid lines) and with $\nu = 0.499$ (dashed lines) for the cases: $\varepsilon_{ri} = 2$ (curves 1 and 5), $\varepsilon_{ri} = 4$ (curves 2 and 6), $\varepsilon_{ri} = 6$ (curves 3 and 7), $\varepsilon_{ri} = 7$ (curves 4 and 8)

Conclusions.

1. A numerical field mathematical 2D model was developed, which consists of sequentially solved equations of electrostatics and structural mechanics for determining the distribution of mechanical stresses in an insulating material with a liquid or gaseous defect and implemented in COMSOL. The adequacy of the model is confirmed by comparison with results known in the literature.

2. The minimum ratio of the maximum stresses in the insulating materials around the surface cracks and pores for ionized air was 9.3 times for the maximum ratio of the major and minor semi-axes of the cross-section of the defect $k = 10$ considered in the work. For the water defect, the similar ratio was 2...5 .6 times, increasing when the relative dielectric permittivity of the insulating material changes from 7 to 2.

3. When the Young modulus of the insulating material increases from 1 MPa to 100 GPa, the angles of inclination to the axis of the ratio of the major and minor semi-axes of the defect cross-section of the linearized dependencies of the maximum mechanical stresses around the limited pores with ionized air (water) increase by 35.9° (58.0 °) and 18.6° (20.1°) at orientations of major semi-axes at angles of 0° and 45°, respectively.

4. The further direction of research consists in establishing the dependencies of the distribution of mechanical stresses in insulating materials with defects based on an improved mathematical model, taking into account the additional spatial coordinate and anisotropy of the physical properties of the materials of the model.

Conflict of interest. The author of the article declares no conflict of interest.

REFERENCES

1. Zhou T., Zhu X., Yang H., Yan X., Jin X., Wan Q. Identification of XLPE cable insulation defects based on deep learning. *Global Energy Interconnection*, 2023, no. vol. 6, no. 1, pp. 36-49. doi: https://doi.org/10.1016/j.gloei.2023.02.004.

2. Qu Z., Zhang G., Fu Y., An Y., Chen C., Shan X. Defect detection for the insulation layer of bent aircraft cables based on ultrasonic guided waves. *IEEE Transactions on Instrumentation and Measurement*, 2023, vol. 72, pp. 1-8. doi: https://doi.org/10.1109/TIM.2023.3241040.

3. Zhou X., Tian T., Li X., Chen K., Luo Y., He N., Liu W., Ma Y., Bai J., Zhang X. and Zhang G. Study on insulation defect discharge features of dry-type reactor based on audible acoustic. *AIP Advances*, 2022, vol. 12, no. 2, art. no. 025210. doi: https://doi.org/10.1063/5.0078735.

4. Wang Y., Nie Y., Qi P., Zhang N., Ye C. Inspection of defect under thick insulation based on magnetic imaging with TMR array sensors. *IEEE Transactions on Magnetics*, 2021, vol. 58, no. 3, art. no. 6200510. doi: https://doi.org/10.1109/TMAG.2021.3138587.

5. Palchykov O.O. Breakdown voltage of micron range air inclusions in capacitor paper. *Electrical Engineering & Electromechanics*, 2020, no. 6, pp. 30-34. doi: https://doi.org/10.20998/2074-272X.2020.6.05.

6. Li G., Liang X., Zhang J., Li X., Wei Y., Hao C. Insulation properties and interface defect simulation of distribution network cable accessories under moisture condition. *IEEE Transactions on Dielectrics and Electrical Insulation*, 2022, vol. 29, no. 2, pp. 403-411. doi: https://doi.org/10.1109/TDEI.2022.3157902.

7. Vavilova G., Yurchenko V., Keyan L. Influence of the insulation defects size on the value of the wire capacitance. *Progress in Material Science and Engineering, Part of the Studies in Systems, Decision and Control book series* (SSDC), 2021, no. 351, pp. 113-123. doi: https://doi.org/10.1007/978-3-030-68103-6_11.

8. Ndama A.T., Ndong E.O., Boussougou Y.C.M., Tsoumou G.J., Blampain E.J.J. Theoretical Study of Potential Manufacturing Insulation Defects in Medium–Voltage Traction Motors. *International Journal of Emerging Technology and Advanced Engineering*, 2022, vol. 12, no. 1, pp. 83-98. doi: https://doi.org/10.46338/ijetae0122_09.
9. Uydur C.C., Arikan J., Kalenderli Ö. The effect of insulation defects on electric and magnetic field distributions in power cables. *Tehnicki Vjesnik*, 2021, vol. 28, no. 4, pp. 1152-1160. doi: https://doi.org/10.17559/TV-20200205084232.
10. Han W., Yang G., Hao C., Wang Z., Kong D. and Dong Y. A data-driven model of cable insulation defect based on convolutional neural networks. *Applied Sciences*, 2022, vol. 12, no. 16, art. no. 8374. doi: https://doi.org/10.3390/app12168374.
11. Zeller H.R., Schneider W.R. Electrofracture mechanics of dielectric aging. *Journal of Applied Physics*, 1984, vol. 56, no. 2, pp. 455-459. doi: https://doi.org/10.1063/1.333931.
12. Scanavi G.I. *Physics of dielectrics (region of strong fields)*. Moscow, GIFML Publ., 1958. 909 p. (Rus).
13. Blythe T., Bloor D. *Electrical properties of polymers.* Cambridge University Press, 2008. 496 p.
14. Zhou X., Zhao X., Suo Z., Zou C. Electrical breakdown and ultrahigh electrical energy density in poly (vinylidene fluoride-hexafluoropropylene) copolymer. *Applied Physics Letters*, 2009, vol. 94, no. 16, art. no. 162901. doi: https://doi.org/10.1063/1.3123001.
15. Karpov V.G., Kryukov Y.A., Karpov I.V., Mitra M. Field-induced nucleation in phase change memory. *Physical Review B*, 2008, vol. 78, no. 5, art. no. 052201. doi: https://doi.org/10.1103/PhysRevB.78.052201.
16. Montanari G.C., Seri P., Dissado L.A. Aging mechanisms of polymeric materials under DC electrical stress: A new approach and similarities to mechanical aging. *IEEE Transactions on Dielectrics and Electrical Insulation*, 2019, vol. 26, no. 2, pp. 634-641. doi: https://doi.org/10.1109/TDEI.2018.007829.
17. Ding H.-Z., Varlow B.R. Thermodynamic model for electrical tree propagation kinetics in combined electrical and mechanical stresses. *IEEE Transactions on Dielectrics and Electrical Insulation*, 2005, vol. 12, no. 1, pp. 81-89. doi: https://doi.org/10.1109/TDEI.2005.1394018.
18. Pallon L.K.H., Nilsson F., Yu S., Liu D., Diaz A., Holler M., Chen X.R., Gubanski S., Hedenqvist M.S., Olsson R.T., Gedde U.W. Three-Dimensional Nanometer Features of Direct Current Electrical Trees in Low-Density Polyethylene. *Nano Letters*, 2017, vol. 17, no. 3, pp. 1402-1408. doi: https://doi.org/10.1021/acs.nanolett.6b04303.
19. Kitani R., Iwata S., Imatani S. Energy-Release Rate in Electrically Deteriorated Materials Introduced by Using Maxwell Stress Tensor at Crack Tip. *IEEE Transactions on Dielectrics and Electrical Insulation*, 2021, vol. 28, no. 6, pp. 1925-1932. doi; https://doi.org/10.1109/TDEI.2021.009692.
20. Zuoqian Wang, Marcolongo P., Lemberg J.A., Panganiban B., Evans J.W., Ritchie R.O., Wright P.K. Mechanical fatigue as a mechanism of water tree propagation in TR-XLPE. *IEEE Transactions on Dielectrics and Electrical Insulation*, 2012, vol. 19, no. 1, pp. 321-330. doi: https://doi.org/10.1109/TDEI.2012.6148534.
21. Kucheriava I.M. Computer analysis of electromechanical stress in polyethylene insulation of power cable at available micro-inclusion. *Technical Electrodynamics*, 2012, no. 5, pp. 10-16. (Rus).
22. Podoltsev O.D., Kucheriava I.M. Multiphysics processes in the region of inclusion in polyethylene insulation of power cable (three-dimensional modeling and experiment). *Technical Electrodynamics*, 2015, no. 3, pp. 3-9. (Rus).
23. Bezprozvannych G.V., Mirchuk I.A. Correlation between electrical and mechanical characteristics of cables with radiation-modified insulation on the basis of a halogen-free polymer composition. *Electrical Engineering & Electromechanics*, 2018, no. 4, pp. 54-57. doi: https://doi.org/10.20998/2074-272X.2018.4.09.
24. Bezprozvannych G.V., Boyko A.N., Roginskiy A.V. Effect of a dielectric barrier on the electric field distribution in high-voltage composite insulation of electric machines. *Electrical Engineering & Electromechanics*, 2018, no. 6, pp. 63-67. doi: https://doi.org/10.20998/2074-272X.2018.6.09.
25. Bezprozvannych G.V., Kyessayev A.G., Mirchuk I.A., Roginskiy A.V. Identification of technological defects in high-voltage solid insulation of electrical insulation structures on the characteristics of partial discharges. *Electrical Engineering & Electromechanics*, 2019, no. 4, pp. 53-58. doi: https://doi.org/10.20998/2074-272X.2019.4.08
26. Abrate S. Criteria for Yielding or Failure of Cellular Materials. *Journal of Sandwich Structures & Materials*, 2008, vol. 10, no. 1, pp. 5-51. doi: https://doi.org/10.1177/1099636207070997.
27. Stratton J.A. *Electromagnetic Theory*. Hoboken, IEEE Press, 2007. 630 p.
28. Lurie A. I. *Theory of Elasticity*. Heidelberg, Springer-Verlag Berlin, 2005. 1050 p.

Received 24.04.2023
Accepted 02.08.2023
Published 02.01.2024

O.O. Palchykov[1]*, PhD,*
[1] Admiral Makarov National University of Shipbuilding,
9, Heroyiv Ukraine Ave, Mykolaiv, 54025, Ukraine,
e-mail: ole2012hulk@gmail.com

How to cite this article:
Palchykov O.O. Determination of the maximum mechanical stresses in the insulating material around a defect with a high dielectric permittivity in an electrostatic field. *Electrical Engineering & Electromechanics*, 2024, no. 1, pp. 69-76. doi: https://doi.org/10.20998/2074-272X.2024.1.09